Advanced characterization of multicaloric materials in pulsed magnetic fields

Gottschall, T.; Bykov, E.; Gràcia-Condal, A.; Beckmann, B.; Taubel, A.; Pfeuffer, L.; Gutfleisch, O.; Manosa, L.; Planes, A.; Scurschii, I.; Wosnitza, J.;

Originally published:

May 2020

Journal of Applied Physics 127(2020), 185107

DOI: https://doi.org/10.1063/5.0006079

Advanced characterization of multicaloric materials in pulsed magnetic fields

T. Gottschall,[1, a)] E. Bykov,[1, 2] A. Gràcia-Condal,[3] B. Beckmann,[4] A. Taubel,[4] L. Pfeuffer,[4] O. Gutfleisch,[4] Ll. Mañosa,[3] A. Planes,[3] Y. Skourski,[1] and J. Wosnitza[1, 2]

[1)] *Dresden High Magnetic Field Laboratory (HLD-EMFL) and Würzburg-Dresden Cluster of Excellence ct.qmat, Helmholtz-Zentrum Dresden-Rossendorf, 01328 Dresden, Germany*

[2)] *Institut für Festkörper- und Materialphysik, Technische Universität Dresden, 01069 Dresden, Germany*

[3)] *Departament de Física de la Matèria Condensada, Facultat de Física, Universitat de Barcelona, 08028 Barcelona, Catalonia, Spain*

[4)] *Institut für Materialwissenschaft, Technical University of Darmstadt, 64287 Darmstadt, Germany*

(Dated: 15 April 2020)

The multicaloric effect is described by a temperature or entropy change of a material triggered by external stimuli applied or removed simultaneously or sequentially. The prerequisite for this is a material exhibiting multiple ferroic states. However, direct measurements of the effect are rarely reported. Now for this reason, we built a measurement device allowing to determine the adiabatic temperature change in pulsed magnetic fields and, simultaneously, under the influence of uniaxial load. We selected the all-*d*-metal Heusler alloy Ni-Mn-Ti-Co for our first tests because of its enhanced mechanical properties and enormous magneto- and elastocaloric effects. Ni-Mn-Ti-Co was exposed to pulsed magnetic fields up to 10 T and uniaxial stresses up to 80 MPa and the corresponding adiabatic temperature changes were measured. With our new experimental tool, we are able to better understand multicaloric materials and determine their cross-coupling responses to different stimuli.

I. INTRODUCTION

Magnetic cooling is a refrigeration technique that is based on the so-called magnetocaloric effect, the change in temperature of a material caused by a magnetic field[1–3]. Besides the magnetocaloric cooling[4–6], there are also other effects that can be utilized for solid-state refrigeration, namely the baro-[7–9], elasto-[10–12], and electrocaloric effects[13,14]. They describe a temperature change induced by an external stimulus, such as hydrostatic pressure, uniaxial load, or an electric field, respectively. In most cases, one requires a ferroic material that is susceptible to an external stimulus. In many materials, these ferroic states are coupled as, for instance, in ferromagnets that are also ferroelastic. In general, they are referred to as multiferroic materials and their change of temperature caused by several fields is described by the multicaloric effect[15–18].

The coupling between the different order parameters is the origin for the multifunctionality of these materials. However, their experimental characterization is challenging, which can often only be done in purpose-built measurement devices and, because of the multidimensionality of the phase diagram, these measurements are very time consuming. For this reason, there are not many reports in the literature on the fascinating properties of multicaloric materials[19–22]. Only very few multiferroics are known that are magnetoelectric and those that do exist often show only very weak coupling effects. This is in contrast to the group of magnetoelastic materials, especially magnetic shape-memory alloys with a first-order phase transition that involves a strong coupling and which are, therefore, predestined to have large multicaloric effects. However, the existence of thermal hysteresis is inherent in these compounds that undergo a first-order transition. This implies that the transition might not be induced in a cyclic way when the magnetic field change is too small to overcome the hysteresis[23].

Almost all magnetocaloric demonstrators use permanent magnets to provide the field, which limits the practical flux density to about 1 T in such a device[24]. For many materials such as Heusler alloys, this rather small field change is not sufficient to allow a cyclic operation[25]. However, in a multicaloric approach it is possible to bypass the hysteresis with a second stimulus, for instance, hydrostatic pressure, whereby the effective driving force becomes larger[26–28]. Another approach is to exploit the thermal hysteresis of first-order materials in a multicaloric cooling cycle instead of avoiding it[29]. In the hysteresis-positive approach, the magnetic field needs to be sufficiently high to transform the material completely. Then, due to the appropriately tuned thermal hysteresis, the reverse transition does not take place during demagnetization. After locking the material in the ferromagnetic phase, the heat can be extracted from the cooling compartment in the absence of the magnetic field. To return the material to its original state, a loading unit is required. The great advantage of the exploiting hysteresis cycle compared to a conventional magnetocaloric one is that the irreversibility of the magnetostructural transition allows reducing the magnetized volume to a minimum, which means that the amount of expensive permanent magnets, and with that the costs, can be reduced drastically. Due to the reduction in the magnetized volume, higher magnetic fields can be generated and thus larger cooling effects can be achieved. However, the exploration of this refrigeration concept as well as multicaloric materials themselves are still at their beginning.

In this work, we have built a new measurement device with

[a)] Electronic mail: t.gottschall@hzdr.de

which we can determine the multicaloric effect of materials directly. We make use of the pulse-field facility at the Dresden High Magnetic Field Laboratory (HLD-EMFL).

II. EXPERIMENTAL DETAILS

As the first object of investigation we have chosen the all-*d*-metal Heusler compound with the nominal composition $Ni_{37.0}Co_{13.0}Mn_{34.5}Ti_{15.5}$. The material was synthesized by arc melting of high-purity elements whereby the ingot was turned several times and melted again. A small part of the Heusler alloy was then brought into cylindrical form by suction casting. Subsequently, the compound was heat treated at a temperature of 1323 K for 96 h followed by quenching in water. The polycrystalline rod with a diameter of 3 mm was then cut into two pieces with heights of 2 and 4 mm which were then polished in order to obtain plane-parallel front surfaces.

Magnetization as a function of temperature in various magnetic fields was measured using a PPMS (Physical Property Measurement System) operated with a heating and cooling rate of $2\,\mathrm{K\,min^{-1}}$. For the measurement of the adiabatic temperature change in pulsed magnetic fields and under constant uniaxial load, we designed an insert that is illustrated in Fig. 1. Main parts of the insert are made of non-magnetic Cu-Be to ensure sufficient mechanical stability. In the current investigation, we placed the thermocouple (not shown in Fig. 1) between the two pieces of the sample bonded with silver epoxy in order to achieve best thermal response. The differential thermocouple was made from copper and constantan wires with a thickness of 25 µm. The reference thermocouple junction was placed near a Pt100 thermometer in order to determine the absolute temperature. The length change of the Heusler alloy along the magnetic field and load direction was monitored by a strain gauge with a grid size of $0.78 \times 1.57\,\mathrm{mm^2}$ that was attached to lateral surface of the sample. The strain gauge was read out by means of a Wheatstone bridge circuit. The mechanical load is transmitted to the sample via two pistons made of the high-performance polymer Torlon. The uniaxial load is tuned from the outside (left side in Fig. 1) by a long screw. In order to be able to work in a regime of quasi-constant load, packs of disk springs of stainless steel – in total 160 pieces – were introduced. The back pressure is built up by the closure at the end of the insert. Here, a piezoelectric force sensor of the type CLP/3kN from the company HBM is placed. The sensor charge, that is proportional to the uniaxial load is monitored by a Keithley 6517B Electrometer.

A heater is located below and above the sample. It is controlled by a Lakeshore 350 temperature controller using the reading from the Pt100 thermometer located in close proximity to the sample. To ensure adiabatic conditions, the insert is placed in a high-vacuum tube. Magnetic-field pulses of 2, 5, and 10 T were generated in a solenoid[30,31]. The data was recorded with an oscilloscope with a sampling time of 2 µs. The maximum field is applied in within 13 ms. In order to reset the material, we used the discontinuous measurement protocol as described in Ref. 32. Before the pulse experiment, we heated the sample to 310 K to reach the austenite phase, then we cooled to 235 K to the martensite state and finally we were approaching the target temperature. This ensures the reproducibility of the measurements.

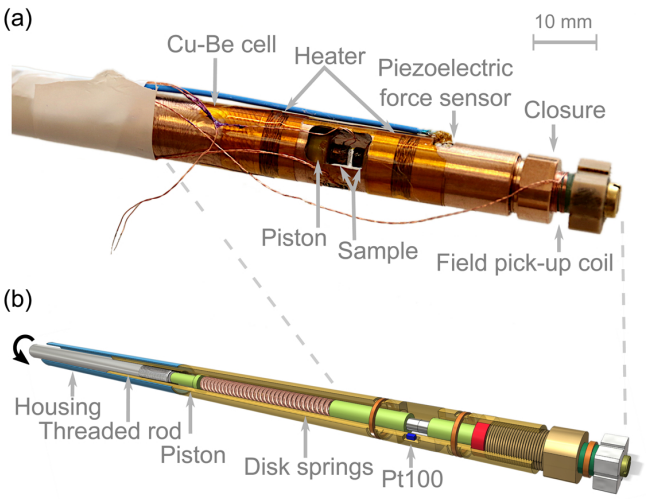

FIG. 1. (a) Photo of the uniaxial load insert for pulsed magnetic fields. The sample is located in the field center of the magnet. The right side of the image corresponds to the bottom of the insert. Both the magnetic field and the uniaxial pressure are directed along the cell. (b) Sketch of the whole insert.

In addition to the pulsed-field experiments, we performed temperature sweeps with a heating and cooling rate of $0.2\,\mathrm{K\,min^{-1}}$ recording the thermoelectric voltage and the strain-gauge resistance with Keithley 2000 Multimeters as well as the force-sensor reading with a Keithley 6517B Electrometer.

III. RESULTS AND DISCUSSION

A. Temperature-driven transition

In Fig. 2, the magnetization of the Heusler alloy $Ni_{37.0}Co_{13.0}Mn_{34.5}Ti_{15.5}$ is plotted as a function of temperature in different magnetic fields showing the typical behavior of inverse magnetocaloric Heusler alloys[33]. The low-temperature martensite phase with low magnetization transforms into the ferromagnetic austenite. This martensitic transition is accompanied by a sharp change of the magnetization. Since a magnetic field favors the phase with higher magnetization – the austenite phase – the transformation shifts towards lower temperatures as the applied magnetic field is increased. On the basis of the magnetization data, linear fits before, in the central part, and after the transition can be used to determine the austenite and martensite start and finish temperatures. This results in an average shift of the transition by about $dT_t/\mu_0 dH = -2.2\,\mathrm{K\,T^{-1}}$ in the considered magnetic fields and a thermal hysteresis of 10 K. Thus the Ni-Mn-Ti-Co sample behaves similar to other Ni-Mn-based Heusler alloys[34].

This value also represents the upper limit for the achievable magnetocaloric effect per field change[35]. The average values for the transformation temperature for heating and cooling in the zero field are 273.6 and 261.3 K, respectively.

In the following, the results of the multicaloric measurement insert are presented. We performed temperature sweeps with a heating and cooling rate of 0.2 K min^{-1} in the absence of a magnetic field and recorded the strain, the force, and the thermoelectric voltage of the thermocouple which is illustrated in Fig. 3. These data sets are useful to characterize the transition under the influence of uniaxial load. The strain as a function of temperature is shown for the stress-free case and for 40 MPa in Fig. 3(a), the strain gauge failed unfortunately for higher loads. Under cooling, the sample shrinks during the martensitic transformation. This effect is related to the change of the crystal symmetry from cubic austenite into tetragonal or monoclinic martensite and the resulting change in volume and length[36]. Without uniaxial load, a strain of about $-0.5\,\%$ appears, whereas a much larger strain of $-1.7\,\%$ is observed under 40 MPa. This effect is caused by the adaptation of the martensite to the stress condition. Martensite variants with their shorter a or b axes aligned along the loading direction are preferred to those oriented with their longer c axis parallel to the pressure direction[37].

This large change of the sample volume and length during the martensitic transition leads to an increase of the transition temperature when being subjected to uniaxial load. It appears, however, that further effects play a role when stress is applied. In addition to a shift, we also observe an enormous broadening of the transition which is nicely seen in Fig. 3(b). In this diagram, the signal of the thermocouple that was contacted to the sample is shown as a function of temperature. From these baseline-subtracted curves for heating and cooling, we obtain information similar as from differential thermal analysis (DTA). A relatively sharp peak is visible in the stress-free case [red curves in Fig. 3(b)]. This is caused by the latent heat that must be absorbed or released during the transition. With increasing uniaxial load, the peak maximum shifts towards higher temperature by about 45 K GPa^{-1} for heating and 55 K GPa^{-1} for cooling.

Further information can be obtained from the piezoelectric force-sensor data shown in Fig. 3(c). Here, the curve in the stress-free case was omitted due to highly noisy data. The dataset shows the shift of the transition towards higher temperatures, which is in good agreement with the strain gauge and thermocouple data. It should be noted that due to the large shrinkage of the sample, the uniaxial load, applied at room temperature, decreases. For the example of 40 MPa, a 20 % reduction of σ by 8 MPa is observed. With a total sample height of 6 mm and a strain of $-1.7\,\%$, the force reduction can be determined based on the spring constant of the disk spring stack, $k \approx 625\,\mathrm{N\,mm^{-1}}$. Based on the diameter of the sample of 3 mm, the theoretical change of the uniaxial load is 8.8 MPa being in very good agreement with the measurement. Due to the limited installation space, it is therefore not possible to ensure conditions of constant load with such large strains. However, the force sensor can be used to estimate the shrinkage of the sample under a load 80 MPa to a value of $-3.4\,\%$, which is in agreement with information from the literature[38].

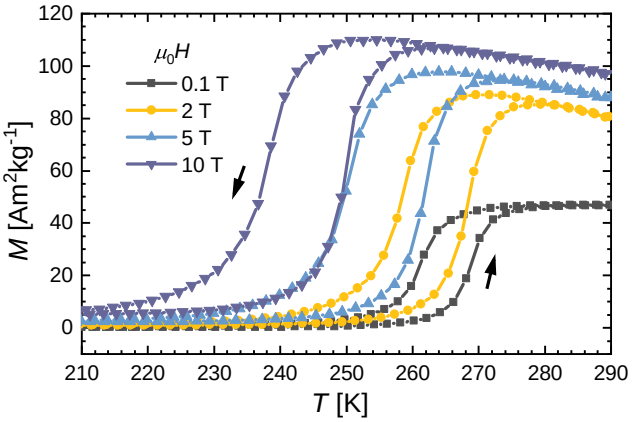

FIG. 2. Magnetization of the Heusler alloy $Ni_{37.0}Co_{13.0}Mn_{34.5}Ti_{15.5}$ as a function of temperature in static magnetic fields of 0.1, 2, 5, and 10 T.

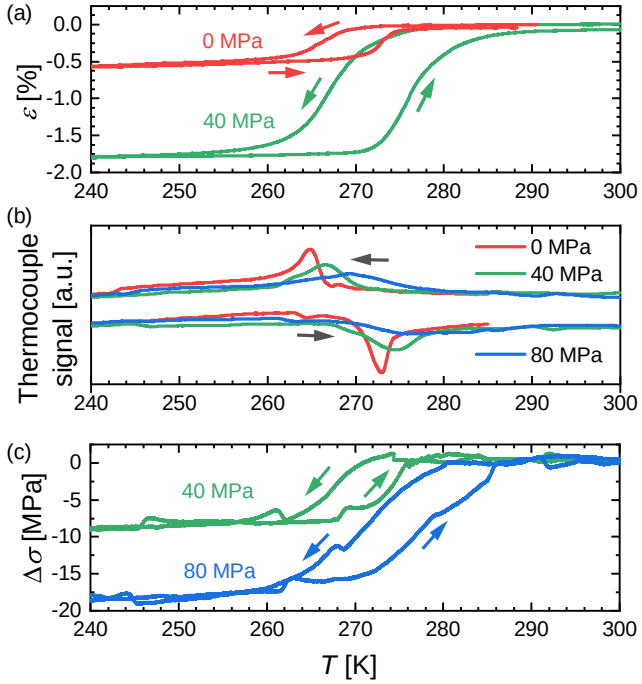

FIG. 3. (a) Strain ε for heating and cooling as a function of temperature without a mechanical load applied and in 40 MPa. (b) Thermocouple signal which allows an estimate of the transition temperature and the width of the transition. (c) Signal of the force sensor that has been normalized to the change of uniaxial load as a function of temperature due to the length change associated with the transition. The sample temperature was changed at a rate of 0.2 K min^{-1}.

B. Magnetic-field-driven transition

The typical time dependence of the pulsed magnetic field is shown in Fig. 4(a). The time to reach the maximum magnetic field is shorter - namely 13 ms - than for the reduction of the field. This shape of the pulse is always the same regardless of the field strength, which results in a maximum field-sweep rate of 1400 T s^{-1} for a 10 T pulse. Despite this rapid field change, the thermocouple reacts quasi instantaneously, which is an indication of good thermal coupling with the sample. In order to erase the memory of the material, we used the discontinuous measurement protocol[32]. Without uniaxial load and at a starting temperature of 265 K, the Heusler alloy cools down by about -17.7 K when being exposed to a magnetic field of 10 T [Fig. 4(b)]. After 100 ms, the field is close to zero again but the temperature does not return to the initial value. This effect is related to the thermal hysteresis of the material resulting in a partial irreversibility of the transition. It is worth noting that the sample temperature remains almost constant at $\Delta T_{ad} = -3.3$ K. If the thermal conduction between the sample and the piston was playing a role on the time scale of a few 100 ms, the temperature would rise again to the initial value. Since this is not the case, this confirms that adiabatic conditions are achieved to a very good extent during the experiment.

Increasing the starting temperature to 270 K (Fig. 4(c)) leads to a slight reduction of the ΔT_{ad} and a plateau evolves indicating that the transition is completed. This will be discussed in more detail later. The final temperature change after the pulse is larger compared to the measurement done at 265 K because of the hysteresis, less material transforms back when being demagnetized. Under a uniaxial load of 40 MPa at the same start temperature [Fig. 4(d)], the adiabatic temperature change is further reduced and also the plateau becomes smaller.

The strain measured during the magnetic-field pulse shows a peculiar behavior [left axes on Figs. 4(b) - (d)]. For a start temperature of 265 K without load, a length change can only be detected 16 ms after the pulse started, that means after the maximum magnetic field has been reached. Then, a rather sharp elongation by 0.8 % is observed, which returns to a value of 0.4 % after a period of rest. In comparison, at a start temperature of 270 K [Fig. 4(c)], there is no strain recovery and the overall length change is much smaller. Under uniaxial load the sample reacts with a small length reduction instead and relaxes back to zero slowly [Fig. 4(d)]. The cause of this length reduction the delay in the three experiments can only be speculated. Even in the stress-free case some residual force is present. The sample is in direct contact with the pistons and the springs behind them (see Fig. 1). Consequently, a large mass has to be moved for a length change of the sample to happen. The inertia of this mass could, therefore, be the reason for the delayed response of the strain gauge. Further studies are required to clarify this behavior.

In the following, we will consider the magnetic-field dependence of the adiabatic temperature change in pulses of 10 T. In Fig. 5(a), at a starting temperature of 265 K, the largest temperature change (ΔT_{ad} value of -17.7 K) is obtained without load (red curve). Comparing the curve shape with earlier

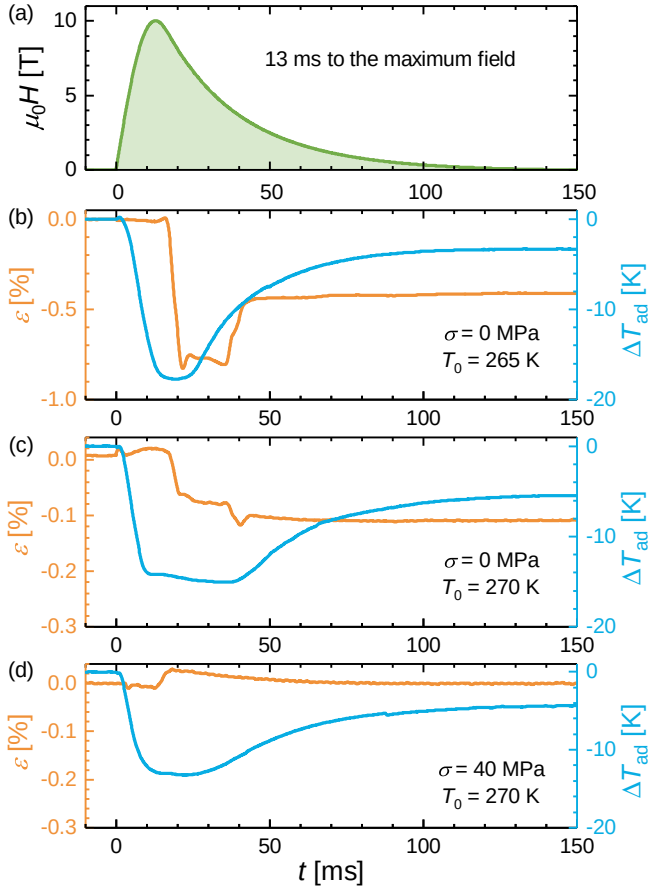

FIG. 4. (a) Time dependence of the magnetic field in the coil. The rise time of the field accounts for 13 ms. (b) - (d) The strain ε of the sample during the experiment is shown on the left and the adiabatic temperature change ΔT_{ad} on the right axes.

works, it seems that the transition is just completed in a field of 10 T[30]. This becomes clearer in Fig. 5(b), where at a start temperature of 270 K the adiabatic temperature change saturates at the maximum field. For the down sweep, the temperature remains almost constant until about 7 T [Fig. 5(a)] or reveals even a slight decrease down to about 4 T, due to the remaining conventional magnetocaloric effect of austenite [Fig. 5(b)] until the backward transition into martensite is initiated. The hysteresis in field accounts for about 5 to 6 T, which is a reasonable result considering a thermal hysteresis of about 10 K and a field-induced shift of the transition temperature of -2.2 K T^{-1}.

For uniaxial stresses of 40 and 80 MPa, the maximum ΔT_{ad} reduces but, notably, the magnetic hysteresis is reduced too. This is mainly caused by the field-decreasing branches – related to the martensite formation – since the curvature for the up sweeps is almost identical in the different examples plotted in Fig. 5. There is no indication of a reduced hysteresis based on our temperature-driven experiments discussed earlier (see Fig. 3). This reduction may be related to minor-loop processes of the hysteresis that work better under uniaxial load but also

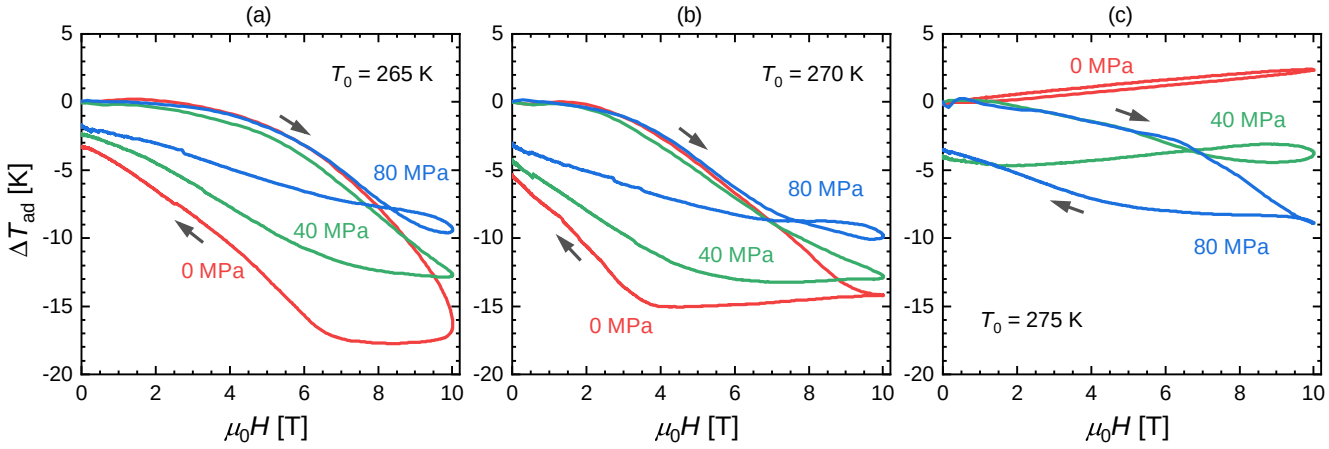

FIG. 5. Magnetic-field-dependent adiabatic temperature change for starting temperatures of (a) 265 K, (b) 270 K, and (c) 275 K in the stress-free case as well as under a uniaxial load of 40 and 80 MPa. The sample was measured in the discontinuous protocol by heating to 310 K and cooling to 235 K before setting the start temperature in order to erase the memory of the transition.

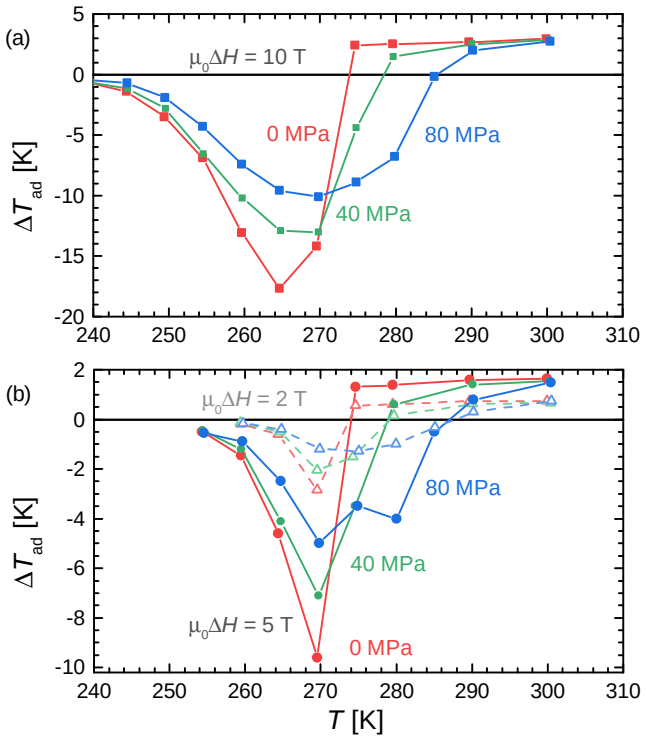

FIG. 6. Adiabatic temperature change ΔT_{ad} in magnetic-field pulses of (a) 10 T and (b) 2 and 5 T for different starting temperatures and uniaxial loads. Negative values of ΔT_{ad} are associated with the field-induced martensitic transition whereas positive temperature changes are caused by the conventional magnetocaloric effect of ferromagnetic austenite.

time-dependent effects of the martensite formation cannot be excluded. In any case, the coupling between the thermocouple and the sample was sufficiently good with and without uniaxial load, which is proven by experiments shown in Fig. 5(c). With zero load and at 275 K, the sample is almost completely in the austenite phase and, consequently, we observe a small conventional magnetocaloric effect with a negligible hysteresis. Therefore, the sample heats up by about 2.4 K in 10 T and cools down reversibly. Under uniaxial load at this start temperature, the material is at least partially in the martensite phase and a field-induced transition takes place. At 80 MPa, there appears even a ΔT_{ad} of -9 K. However, it remains unclear where the change in slope at about 7 T in the up sweep at this load comes from.

In Fig. 6, the adiabatic temperature change at the maximum field of 2, 5, and 10 T pulses is plotted as a function of the start temperature for the three different uniaxial loads. The conventional magnetocaloric effect of the ferromagnetic austenite is not affected by the load at all as can be seen at 300 K. If there is any uniaxial-pressure dependence on the austenitic Curie temperature, which is beyond 340 K, it is not noticable in the adiabatic temperature change near room temperature. For 10 T in the stress-free case, a sharp negative peak with a maximum at 265 K is observed [Fig. 6(a)]. Between 270 and 275 K, the first-order transition is completed and the inverse magnetocaloric effect turns into a small conventional one in the austenite phase. By applying uniaxial pressure, the peak height reduces and at the same time it broadens significantly. We find that the load influence on ΔT_{ad} is most pronounced at higher temperatures. Below 255 K, there is almost no difference in ΔT_{ad} between the pulsed-field measurements at different loads. In 2 and 5 T [Fig. 6(b)], a very similar picture emerges as for the 10 T case.

Two effects play a decisive role in explaining the observed behavior. The broadening of the transition under the influence of uniaxial load can be attributed to the formation of heterogeneous mechanical-stress fields as has been reported for other shape-memory alloys[39,40]. For this reason, certain regions of the sample are subject to a different shift in the transformation temperature in the strained state, which broadens the peak of the magnetocaloric effect and reduces its height. Furthermore,

the shift towards higher temperatures itself causes a weakening of the magnetic contribution to the total entropy. This is why the driving force of the magnetocaloric effect $dT_t/\mu_0 dH$ has to decrease and higher magnetic fields are necessary to fully induce the transition[41]. This also contributes to the decrease of the adiabatic temperature change in the magnetic-field changes under consideration. However, the reduction of the magnetic entropy by uniaxial load must result in an increase of the maximum possible magnetocaloric effect. To observe this behavior, much higher pulsed magnetic fields are required than those applied in this first experiment. We will continue to investigate this aspect in future studies.

IV. CONCLUSION AND OUTLOOK

Using a specially designed device, we could directly determine the multicaloric effect under uniaxial load and pulsed magnetic fields. We were able to show that, despite the technically challenging setup, such measurements are possible with high quality. This can be realized by the short pulse duration of the magnet, which practically prevents heat exchange between sample and piston during the pulse. However, the large sample size that we used and especially its large transformation strain of several percent led to a load change of about 20 %. Nonetheless, for the investigated Heusler alloy we could show a very decisive influence of the uniaxial load on the transformation characteristics and on the adiabatic temperature change. For example, the magnetic hysteresis of ΔT_{ad} reduces but at the same time the transition broadens and also the overall effect decreases. This can be attributed both to a reduction of the magnetic contribution to the total entropy and to the formation of heterogeneous stress fields under the influence of uniaxial load.

In the next steps, we will further improve our measurement setup by focussing on the detection of the strain in the sample installed. Another promising goal is to allow for the readout of the piezoelectric force sensor not only under static conditions but also in pulsed fields. Here, we can rely on our in-house experience of polarization measurements on ferroelectric materials. The insert can also be utilized in order to study materials for the exploiting hysteresis cycle. Magnetic field pulses and mechanical load can be applied in an alternating manner with the advantage that the available magnetic field is sufficiently high to transform all candidate materials completely. In any case, the interplay of mechanical stresses and magnetic fields poses many questions for fundamental research and also challenges for transferring this into practical and efficient caloric devices.

ACKNOWLEDGMENTS

We thank O. Kersten, M. Gulich, and R. Sobiella for technical assistance. This work was supported by the European Research Council (ERC) under the European Unions Horizon 2020 research and innovation programme (Grant No. 743116-project Cool Innov), the CICyT (Spain) Project MAT2016-75823-R, the Helmholtz Association via the Helmholtz-RSF Joint Research Group with the Project No. HRSF-0045, the HLD at HZDR, a member of the European Magnetic Field Laboratory (EMFL), from the DFG through the Würzburg-Dresden Cluster of Excellence on Complexity and Topology in Quantum Matter – *ct.qmat* (EXC 2147, project-id 39085490), and from the DFG via the Project-ID 405553726 — TRR 270. A.G. acknowledges financial support from Universitat de Barcelona under the APIF scholarship, and by the EMFL Travel Grant.

[1] O. Gutfleisch, T. Gottschall, M. Fries, D. Benke, I. Radulov, K. P. Skokov, H. Wende, M. Gruner, M. Acet, P. Entel, and M. Farle, "Mastering hysteresis in magnetocaloric materials," Phil. Trans. R. Soc. A **374**, 20150308 (2016).

[2] J. Lyubina, "Magnetocaloric materials for energy efficient cooling," J. Phys. D: Appl. Phys. **50**, 053002 (2017).

[3] V. Franco, J. Blázquez, J. Ipus, J. Law, L. Moreno-Ramírez, and A. Conde, "Magnetocaloric effect: From materials research to refrigeration devices," Prog. Mater Sci. **93**, 112 – 232 (2018).

[4] A. Waske, M. E. Gruner, T. Gottschall, and O. Gutfleisch, "Magnetocaloric materials for refrigeration near room temperature," MRS Bulletin **43**, 269–273 (2018).

[5] L. D. Griffith, Y. Mudryk, J. Slaughter, and V. K. Pecharsky, "Material-based figure of merit for caloric materials," J. Appl. Phys. **123**, 034902 (2018).

[6] A. Bartok, M. Kustov, L. Cohen, A. Pasko, K. Zehani, L. Bessais, F. Mazaleyrat, and M. LoBue, "Study of the first paramagnetic to ferromagnetic transition in as prepared samples of Mn–Fe–P–Si magnetocaloric compounds prepared by different synthesis routes," J. Magn. Magn. Mater. **400**, 333 – 338 (2016).

[7] L. Mañosa, D. González-Alonso, A. Planes, E. Bonnot, M. Barrio, J.-L. Tamarit, S. Aksoy, and M. Acet, "Giant solid-state barocaloric effect in the Ni-Mn-In magnetic shape-memory alloy," Nat. Mater. **9**, 478–481 (2010).

[8] D. Matsunami, A. Fujita, K. Takenaka, and M. Kano, "Giant barocaloric effect enhanced by the frustration of the antiferromagnetic phase in Mn_3GaN," Nat. Mater. **14**, 73–78 (2015).

[9] A. Aznar, A. Gràcia-Condal, A. Planes, P. Lloveras, M. Barrio, J.-L. Tamarit, W. Xiong, D. Cong, C. Popescu, and L. Mañosa, "Giant barocaloric effect in all-*d*-metal Heusler shape memory alloys," Phys. Rev. Materials **3**, 044406 (2019).

[10] E. Bonnot, R. Romero, L. Mañosa, E. Vives, and A. Planes, "Elastocaloric Effect Associated with the Martensitic Transition in Shape-Memory Alloys," Phys. Rev. Lett. **100**, 125901 (2008).

[11] S. Qian, J. Ling, Y. Hwang, R. Radermacher, and I. Takeuchi, "Thermodynamics cycle analysis and numerical modeling of thermoelastic cooling systems," Int. J. Refrig **56**, 65 – 80 (2015).

[12] Y. Qu, A. Gràcia-Condal, L. Mañosa, A. Planes, D. Cong, Z. Nie, Y. Ren, and Y. Wang, "Outstanding caloric performances for energy-efficient multicaloric cooling in a Ni-Mn-based multifunctional alloy," Acta Mater. **177**, 46 – 55 (2019).

[13] J. Scott, "Electrocaloric Materials," Annu. Rev. Mater. Res. **41**, 229–240 (2011).

[14] M. Ožbolt, A. Kitanovski, J. Tušek, and A. Poredoš, "Electrocaloric refrigeration: Thermodynamics, state of the art and future perspectives ," Int. J. Refrig **40**, 174 – 188 (2014).

[15] S. Fähler, U. K. Rößler, O. Kastner, J. Eckert, G. Eggeler, H. Emmerich, P. Entel, S. Müller, E. Quandt, and K. Albe, "Caloric Effects in Ferroic Materials: New Concepts for Cooling," Adv. Eng. Mater. **14**, 10–19 (2012).

[16] X. Moya, E. Defay, V. Heine, and N. D. Mathur, "Too cool to work," Nat. Phys. **11**, 202–205 (2015).

[17] A. Planes, T. Castán, and A. Saxena, "Thermodynamics of multicaloric effects in multiferroics," Philos. Mag. **94**, 1893–1908 (2014).

[18] A. Amirov, V. Rodionov, I. Starkov, A. Starkov, and A. Aliev, "Magnetoelectric coupling in $Fe_{48}Rh_{52}$-PZT multiferroic composite," J. Magn. Magn. Mater. **470**, 77 – 80 (2019).

[19] M. M. Vopson, "Multicaloric effect: An outlook," Physica B **513**, 103 – 105 (2017).

[20] E. Stern-Taulats, T. Castán, A. Planes, L. H. Lewis, R. Barua, S. Pramanick, S. Majumdar, and L. Mañosa, "Giant multicaloric response of bulk $Fe_{49}Rh_{51}$," Phys. Rev. B **95**, 104424 (2017).

[21] A. Czernuszewicz, J. Kaleta, and D. Lewandowski, "Multicaloric effect: Toward a breakthrough in cooling technology," Energy Convers. Manage. **178**, 335 – 342 (2018).

[22] F.-X. Liang, J.-Z. Hao, F.-R. Shen, H.-B. Zhou, J. Wang, F.-X. Hu, J. He, J.-R. Sun, and B.-G. Shen, "Experimental study on coupled caloric effect driven by dual fields in metamagnetic Heusler alloy $Ni_{50}Mn_{35}In_{15}$," APL Mater. **7**, 051102 (2019).

[23] N. M. Bruno, S. Wang, I. Karaman, and Y. I. Chumlyakov, "Reversible Martensitic Transformation under Low Magnetic Fields in Magnetic Shape Memory Alloys," Sci. Rep. **7**, 40434 (2017).

[24] A. Kitanovski, U. Plaznik, U. Tomc, and A. Poredos, "Present and future caloric refrigeration and heat-pump technologies," Int. J. Refrig. **57**, 288 – 298 (2015).

[25] T. Gottschall, K. P. Skokov, M. Fries, A. Taubel, I. Radulov, F. Scheibel, D. Benke, S. Riegg, and O. Gutfleisch, "Making a Cool Choice: The Materials Library of Magnetic Refrigeration," Adv. Energy Mater. **9**, 1901322 (2019).

[26] J. Liu, T. Gottschall, K. P. Skokov, J. D. Moore, and O. Gutfleisch, "Giant magnetocaloric effect driven by structural transitions," Nat. Mater. **11**, 620–626 (2012).

[27] E. Stern-Taulats, T. Castán, L. Mañosa, A. Planes, N. D. Mathur, and X. Moya, "Multicaloric materials and effects," MRS Bulletin **43**, 295–299 (2018).

[28] Y. Qu, D. Cong, S. Li, W. Gui, Z. Nie, M. Zhang, Y. Ren, and Y. Wang, "Simultaneously achieved large reversible elastocaloric and magnetocaloric effects and their coupling in a magnetic shape memory alloy," Acta Mater. **151**, 41 – 55 (2018).

[29] T. Gottschall, A. Gràcia-Condal, M. Fries, A. Taubel, L. Pfeuffer, L. Mañosa, A. Planes, K. P. Skokov, and O. Gutfleisch, "A multicaloric cooling cycle that exploits thermal hysteresis," Nat. Mater. **17**, 929 (2018).

[30] T. Gottschall, K. P. Skokov, F. Scheibel, M. Acet, M. G. Zavareh, Y. Skourski, J. Wosnitza, M. Farle, and O. Gutfleisch, "Dynamical Effects of the Martensitic Transition in Magnetocaloric Heusler Alloys from Direct ΔT_{ad} Measurements under Different Magnetic-Field-Sweep Rates," Phys. Rev. Applied **5**, 024013 (2016).

[31] C. Salazar-Mejía, V. Kumar, C. Felser, Y. Skourski, J. Wosnitza, and A. Nayak, "Measurement-Protocol Dependence of the Magnetocaloric Effect in Ni-Co-Mn-Sb Heusler Alloys," Phys. Rev. Applied **11**, 054006 (2019).

[32] L. Caron, N. B. Doan, and L. Ranno, "On entropy change measurements around first order phase transitions in caloric materials," J. Phys.: Condens. Matter **29**, 075401 (2017).

[33] Z. Y. Wei, W. Sun, Q. Shen, Y. Shen, Y. F. Zhang, E. K. Liu, and J. Liu, "Elastocaloric effect of all-d-metal Heusler NiMnTi(Co) magnetic shape memory alloys by digital image correlation and infrared thermography," Appl. Phys. Lett. **114**, 101903 (2019).

[34] A. Taubel, T. Gottschall, M. Fries, S. Riegg, C. Soon, K. P. Skokov, and O. Gutfleisch, "A Comparative Study on the Magnetocaloric Properties of Ni-Mn-X(-Co) Heusler Alloys," Phys. Status Solidi B **255**, 1700331 (2017).

[35] K. P. Skokov, V. V. Khovaylo, K.-H. Müller, J. D. Moore, J. Liu, and O. Gutfleisch, "Magnetocaloric materials with first-order phase transition: thermal and magnetic hysteresis in $LaFe_{11.8}Si_{1.2}$ and $Ni_{2.21}Mn_{0.77}Ga_{1.02}$ (invited)," J. Appl. Phys. **111**, 07A910 (2012).

[36] Z. Y. Wei, E. K. Liu, J. H. Chen, Y. Li, G. D. Liu, H. Z. Luo, X. K. Xi, H. W. Zhang, W. H. Wang, and G. H. Wu, "Realization of multifunctional shape-memory ferromagnets in all-d-metal Heusler phases," Appl. Phys. Lett. **107**, 022406 (2015).

[37] R. Tickle and R. James, "Magnetic and magnetomechanical properties of Ni_2MnGa," J. Magn. Magn. Mater. **195**, 627 – 638 (1999).

[38] D. Cong, W. Xiong, A. Planes, Y. Ren, L. Mañosa, P. Cao, Z. Nie, X. Sun, Z. Yang, X. Hong, and Y. Wang, "Colossal Elastocaloric Effect in Ferroelastic Ni-Mn-Ti Alloys," Phys. Rev. Lett. **122**, 255703 (2019).

[39] G. S. Bigelow, S. A. Padula, A. Garg, D. Gaydosh, and R. D. Noebe, "Characterization of Ternary NiTiPd High-Temperature Shape-Memory Alloys under Load-Biased Thermal Cycling," Metall. and Mat. Trans. A **41**, 3065–3079 (2010).

[40] Z. Yang, D. Cong, L. Huang, Z. Nie, X. Sun, Q. Zhang, and Y. Wang, "Large elastocaloric effect in a Ni–Co–Mn–Sn magnetic shape memory alloy," Mater. Des. **92**, 932 – 936 (2016).

[41] T. Gottschall, K. P. Skokov, D. Benke, M. E. Gruner, and O. Gutfleisch, "Contradictory role of the magnetic contribution in inverse magnetocaloric Heusler materials," Phys. Rev. B **93**, 184431 (2016).